Label Distribution Learning with Biased Annotations Assisted by Multi-Label Learning

Zhiqiang Kou[1,2,3] , **Si Qin**[1,2] , **Hailin Wang**[6] , **Jing Wang**[1,2] , **Mingkun Xie**[3] , **Shuo Chen**[3] ,
Yuheng Jia[1,2] **Tongliang Liu**[5] , **Masashi Sugiyama**[3,4] and **Xin Geng**[1,2]

[1]School of Computer Science and Engineering, Southeast University, China
[2]Key Laboratory of New Generation Artifcial Intelligence Technology and Its Interdisciplinary
Applications (Southeast University), Ministry of Education, China
[3]RIKEN Center for Advanced Intelligence Project, Tokyo 103-0027, Japan
[4]Graduate School of Frontier Sciences, The University of Tokyo, Japan
[5]Sydney AI Centre, The University of Sydney, Australia
[6]School of Mathematics and Statistics, Xi'an Jiaotong University, China
{zhiqiang.kou, wangjing91, yhjia, xgeng}@seu.edu.cn, siqin.seu@gmail.com
{ming-kun.xie, shuo.chen.ya}@riken.jp, wanghailin97@163.com
liu@sydney.edu.au,sugi@k.u-tokyo.ac.jp

Abstract

Multi-label learning (MLL) has gained attention for its ability to represent real-world data. Label Distribution Learning (LDL), an extension of MLL to learning from label distributions, faces challenges in collecting accurate label distributions. To address the issue of biased annotations, based on the low-rank assumption, existing works recover true distributions from biased observations by exploring the label correlations. However, recent evidence shows that the label distribution tends to be full-rank, and naive apply of low-rank approximation on biased observation leads to inaccurate recovery and performance degradation. In this paper, we address the LDL with biased annotations problem from a novel perspective, where we first degenerate the soft label distribution into a hard multi-hot label and then recover the true label information for each instance. This idea stems from an insight that assigning hard multi-hot labels is often easier than assigning a soft label distribution, and it shows stronger immunity to noise disturbances, leading to smaller label bias. Moreover, assuming that the multi-label space for predicting label distributions is low-rank offers a more reasonable approach to capturing label correlations. Theoretical analysis and experiments confirm the effectiveness of our method on real-world datasets.

1 Introduction

Multi-Label Learning (MLL) [Zhang and Zhou, 2014] has gained significant attention due to its ability to associate multiple labels with a single instance, making it widely applicable in tasks such as text classification [Liu *et al.*, 2017] and image annotation [Jing *et al.*, 2016].

Label Distribution Learning (LDL)[1] [Geng, 2016] extends MLL by assigning a real-valued *label description degree* [Jia *et al.*, 2019] to each label, offering more detailed supervisory information. Leveraging label correlations is a key strategy in MLL [Huang and Zhou, 2012], and applying low-rank constraints in the output space is an effective approach to capturing these correlations [Zhu *et al.*, 2017]. Building on the advancements in label correlation modeling in MLL, a branch of algorithms [Jia *et al.*, 2018][Jia *et al.*, 2019][Kou *et al.*, 2023] has extended these techniques to LDL by assuming low-rank structures in label distribution spaces, aiming to capture label correlations more comprehensively.

Annotating label distributions is inherently challenging and often leads to *biased label distributions*, where the collected label distributions deviate from the true distributions due to variations in annotators' expertise or subjective judgments[Xie and Huang, 2018]. The existing method [He *et al.*, 2024] [Kou *et al.*, 2024a] [Xu and Zhou, 2017] aims to address this issue by leveraging label correlations modeling the clean label distribution and training LDL models effectively. For instance, IncomLDL [Xu and Zhou, 2017] aims to model the learned label distribution space using low-rank label correlations, thereby completing the missing entries in the label distribution matrix. And in LRS-LDL[Kou *et al.*, 2023], the noisy label distribution is modeled as $\hat{\mathbf{D}} = \mathbf{D} + \mathbf{E}$, where $\mathbf{D}$ is the true label distributions and $\mathbf{E}$ represents noise. It assumes a low-rank structure on the output space ($\mathbf{D} = \mathbf{WX}$) and sparsity of the noise. Similarly, IDI-LDL [Kou *et al.*, 2024a] applies a low-rank assumption on the output space while employing an $\ell_{2,1}$-norm constraint on the noise.

However, recent evidence shows that the label distribution

---

[1]LDL is similar to learning from soft labels, but the soft-label formulation focuses on single-label problems (i.e., there is only one true label for each instance), while LDL considers multi-label problems (i.e., each instance can have multiple true labels).

Biased Label Distribution $\hat{D}$

Sad	Fear	Joy	Surprise	Netural
0.39	0.44	0	0.17	0

degenerate

Muti-label $\hat{L}$

Sad	Fear	Joy	Surprise	Netural
1	1	0	0	0

$$\delta_1 = d(\hat{D}, D) \gg d(\hat{L}, L) = \delta_2$$

Sad	Fear	Joy	Surprise	Netural
0.43	0.48	0	0.09	0

True Label Distribution D

Sad	Fear	Joy	Surprise	Netural
1	1	0	0	0

Muti-label L

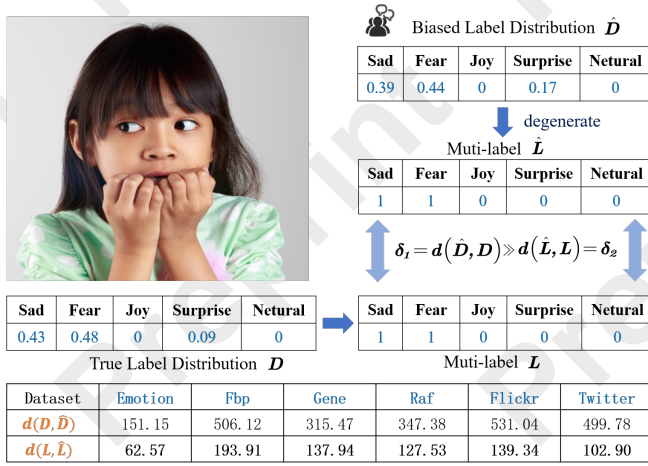| Dataset	Emotion	Fbp	Gene	Raf	Flickr	Twitter
$d(D, \hat{D})$	151.15	506.12	315.47	347.38	531.04	499.78
$d(L, \hat{L})$	62.57	193.91	137.94	127.53	139.34	102.90

Figure 1: Illustration of biased label distribution learning using examples from the RAF dataset [Li and Deng, 2019]. Despite discrepancies between the biased label distribution $\hat{D}$ and the true distribution D, their corresponding multi-label representations ($\hat{L}$ and L) are much closer.

tends to be full-rank [Wang and Geng, 2021], and naive apply of low-rank approximation on biased observation leads to inaccurate recovery and performance degradation. In this paper, we address the LDL with biased annotations problem from a novel perspective, where we first degenerate the soft label distribution into a hard multi-hot label and then recover the true label information for each instance. This idea stems from an insight that assigning hard multi-hot labels is often easier than assigning a soft label distribution, and it shows stronger immunity to noise disturbances, leading to smaller label bias. As shown in Fig. 1, one images from the Real-world Affective Faces (RAF) [Li and Deng, 2019] reveals significant discrepancies between the biased and true soft label distributions ($\hat{D}$ and D). However, their corresponding multi-hot label ($\hat{L}$ and L) exhibit much smaller differences. This phenomenon holds across datasets, as demonstrated by the Tables in Fig. 1. Moreover, while label distributions are inherently full-rank [Wang and Geng, 2021], multi-label spaces are widely regarded as low-rank [Zhu et al., 2017], making them more computationally efficient for correlation modeling. The contributions of this work are summarized as

- We utilize multi-label information and label correlations to model the recovery of the true label distribution and propose the BLDL algorithm (Sections 2).
- Extensive theoretical analysis is provided, including convergence guarantees and generalization error bounds (Section 4).
- The effectiveness of the method is validated through comprehensive experiments, with superior performance demonstrated and insights verified. (Section 5).

1.1 Preliminaries

Denote $\mathbf{X} \in \mathbb{R}^{d \times n}$ as the feature matrix, where d is the feature dimensionality and n is the number of instances. The label space is $\mathcal{Y} = \{y_1, \ldots, y_m\}$, where m is the number of la-

bels. The accurate training set for LDL is $\mathcal{T} = \{(\mathbf{x}_i, \mathbf{d}_i)\}_{i=1}^n$, with $\mathbf{d}_i = [d_{\mathbf{x}_i}^{y_1}, \cdots, d_{\mathbf{x}_m}^{y_m}]^\top \in \mathbb{R}^m$, satisfying $d_{\mathbf{x}_i}^y \geq 0$ for all $y \in \mathcal{Y}$ and $\sum_y d_{\mathbf{x}_i}^y = 1$. The label distribution matrix is $\mathbf{D} = [\mathbf{d}_1, \ldots, \mathbf{d}_n] \in \mathbb{R}^{m \times n}$. We assume the observed label distribution $\hat{\mathbf{D}} \in \mathbb{R}^{m \times n}$ is biased, while the true label distribution is unknown. The goal is to learn a decision function $\mathfrak{G} : \mathbb{R}^{d \times n} \to \mathbb{R}^{m \times n}$ using the training set $\{\mathbf{X}, \hat{\mathbf{D}}\}$, such that $\mathfrak{G}(\mathbf{X}_{i:}) \approx \mathbf{D}_{i:}$.

2 The BLDL Approach

A common approach in multi-label learning to capture label correlations is leveraging low-rank modeling on the output space. This can be formulated as the following optimization problem:

$$\min_{\mathbf{W}} \ \text{rank}(\mathbf{WX}), \quad \text{s.t.} \ \|\mathbf{WX} - \mathbf{L}\|_F \leq \delta, \qquad (1)$$

where $\mathbf{W} \in \mathbb{R}^{m \times d}$ is the learned weight matrix mapping the feature space to the multi-label space $\mathbf{L} \in \mathbb{R}^{m \times n}$. The first term captures label correlations via low-rank modeling [Jia et al., 2019].

Annotating label distributions is challenging, often introducing bias. As an extension of MLL, certain bias LDL methods leverage label correlations to recover true distributions from biased ones while learning an effective model. These methods can be formulated as:

$$\min_{\mathbf{W}, \mathbf{D}, \mathbf{E}} \ \text{rank}(\mathbf{WX}) + \mathcal{R},$$
$$\text{s.t.} \ \|\mathbf{WX} - \mathbf{D}\|_F \leq \delta_1, \| \hat{\mathbf{D}} - \mathbf{D} + \mathbf{E}\| \leq \delta_2, \qquad (2)$$

where $\mathbf{D} \in \mathbb{R}^{m \times n}$ is the recovered label distribution, $\mathbf{E} \in \mathbb{R}^{m \times n}$ is the annotation bias, and $\mathcal{R}$ applies regularization. δ_1 and δ_2 represent the reconstruction errors in the optimization process.

However, recent evidence shows that the label distribution tends to be *full-rank* [Wang and Geng, 2021], and naive apply of low-rank approximation on biased observation leads to *inaccurate recovery and performance degradation*. In this paper, we address the above limitations of existing methods. Our method are enhance as below:

$$\min_{\mathbf{W}, \mathbf{O}, \mathbf{D}} \ \text{rank}(\mathbf{WXO}) + \alpha \|\hat{\mathbf{D}}\mathbf{O} - \hat{\mathbf{L}}\|_F$$
$$+ \beta \|\mathbf{WX} - \mathbf{D}\|_F + \lambda_1 \|\mathbf{W}\|_F^2 + \lambda_2 \|\mathbf{O}\|_F^2, \qquad (3)$$
$$\text{s.t.} \|\hat{\mathbf{D}} - \mathbf{D}\|_F \leq \delta_1, \quad \|\mathbf{DO} - \hat{\mathbf{L}}\|_F \leq \delta_2,$$

where $\mathbf{O} \in \mathbb{R}^{m \times m}$ models the degradation from label distribution to multi-label, and $\hat{\mathbf{L}} \in \mathbb{R}^{m \times n}$ represents the multi-label derived from biased distribution. $\mathbf{D}$ is recovered label distribution. Parameters α, β, and λ_i control the term weightings. Our method consists of three parts. The *first part* is label distribution recovery, where we use both the biased label distribution and its multi-label representation. Recovering the label distribution via the multi-label space is more reliable than relying directly on the biased distribution, as the discrepancy between the biased and true distributions is much larger than between their multi-label representations. By constraining the degradation of the recovered true distribution to the multi-label space (Condition 2), the reliability of the process is ensured. We also require that the difference between
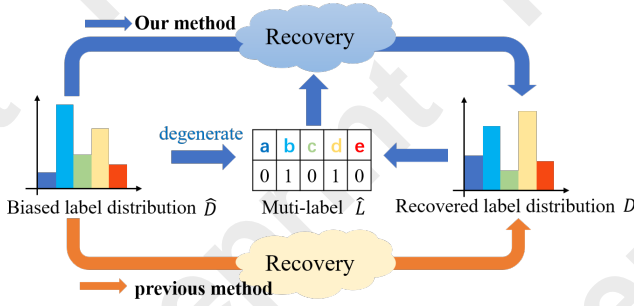
Figure 2: An overview of the proposed BLDL framework.

the recovered true distribution and the biased distribution be bounded by δ_1 (Condition 1) to control the recovery of the label distribution. The *second part* is label distribution learning, where we impose a low-rank constraint on the multi-label space (instead of the label distribution space, since it is full-rank) to capture label correlations (the first, third, and fourth terms of Eq. (3)). The *final part* is the multi-label mapping process, where we learn the mapping from multi-labels to label distributions (the second and fifth terms of Eq. (3)). The algorithm flow chart is shown in Fig. 2,

3 Optimization

To solve model (3), we relax the rank by its convex alternative, nuclear norm [Gu *et al.*, 2014], and then apply the ADMM [Boyd *et al.*, 2011] for efficient optimization. The corresponding augmented Lagrangian function is:

$$
\begin{aligned}
&\mathcal{L}(\mathbf{W}, \mathbf{O}, \mathbf{D}, \mathbf{Z}, \mathbf{\Lambda}) \\
&= \|\mathbf{Z}\|_* + \alpha\|\mathbf{WX} - \mathbf{D}\|_F^2 + \beta\|\hat{\mathbf{D}}\mathbf{O} - \hat{\mathbf{L}}\|_F^2 \\
&\quad + \gamma\|\mathbf{DO} - \hat{\mathbf{L}}\|_F^2 + \eta\|\mathbf{D} - \hat{\mathbf{D}}\|_F^2 + \lambda_1\|\mathbf{W}\|_F^2 + \lambda_2\|\mathbf{O}\|_F^2 \\
&\quad + \langle \mathbf{\Lambda}, \mathbf{Z} - \mathbf{WXO} \rangle + \frac{\rho}{2}\|\mathbf{Z} - \mathbf{WXO}\|_F^2,
\end{aligned}
$$

where $\mathbf{Z}$ is a splitting variable of $\mathbf{WXO}$, $\mathbf{\Lambda}$ is the Lagrange multiplier, and ρ is positive penalty parameter. The optimization is performed by iteratively updating $\mathbf{W}, \mathbf{O}, \mathbf{D}, \mathbf{Z}, \mathbf{\Lambda}$ as follows:

1) **W-subproblem** is formulated as:

$$
\begin{aligned}
\mathbf{W}^{k+1} = \arg\min_{\mathbf{W}} \; &\alpha\|\mathbf{WX} - \mathbf{D}\|_F^2 + \lambda_1\|\mathbf{W}\|_F^2 \\
&+ \frac{\rho}{2}\|\mathbf{Z} - \mathbf{WXO} + \mathbf{\Lambda}/\rho\|_F^2.
\end{aligned}
$$

To obtain the solution, we set the derivative of the objective with respect to $\mathbf{W}$ to zero, and we get:

$$
\begin{aligned}
\mathbf{W}^{k+1} = &\left(2\alpha\mathbf{DX}^\top + \rho(\mathbf{Z} + \mathbf{\Lambda}/\rho)\mathbf{O}^\top\mathbf{X}^\top\right) \\
&\cdot \left(2\alpha\mathbf{XX}^\top + \rho\mathbf{XOO}^\top\mathbf{X}^\top + 2\lambda_1\mathbf{I}\right)^{-1}.
\end{aligned}
$$

2) **O-subproblem** is formulated as:

$$
\begin{aligned}
\mathbf{O}^{k+1} = \arg\min_{\mathbf{O}} \; &\beta\|\hat{\mathbf{D}}\mathbf{O} - \hat{\mathbf{L}}\|_F^2 + \gamma\|\mathbf{DO} - \hat{\mathbf{L}}\|_F^2 \\
&+ \lambda_2\|\mathbf{O}\|_F^2 + \frac{\rho}{2}\|\mathbf{Z} - \mathbf{WXO} + \mathbf{\Lambda}/\rho\|_F^2.
\end{aligned}
$$

Similar to the solution for $\mathbf{W}$, and we get:

$$
\begin{aligned}
\mathbf{O}^{k+1} = &\left(2\beta\hat{\mathbf{D}}^\top\hat{\mathbf{D}} + 2\gamma\mathbf{D}^\top\mathbf{D} + \rho\mathbf{X}^\top\mathbf{W}^\top\mathbf{WX} + 2\lambda_2\mathbf{I}\right)^{-1} \\
&\cdot \left(2\beta\hat{\mathbf{D}}^\top\hat{\mathbf{L}} + 2\gamma\mathbf{D}^\top\hat{\mathbf{L}} + \rho\mathbf{X}^\top\mathbf{W}^\top(\mathbf{Z} + \mathbf{\Lambda}/\rho)\right).
\end{aligned}
$$

3) **D-subproblem** is formulated as:

$$
\begin{aligned}
\mathbf{D}^{k+1} = \arg\min_{\mathbf{D}} \; &\alpha\|\mathbf{WX} - \mathbf{D}\|_F^2 \\
&+ \gamma\|\mathbf{DO} - \hat{\mathbf{L}}\|_F^2 + \eta\|\mathbf{D} - \hat{\mathbf{D}}\|_F^2.
\end{aligned}
$$

Similar to the solution above, and we get:

$$
\begin{aligned}
\mathbf{D}^{k+1} = &\left(2\alpha\mathbf{WX} + 2\gamma\hat{\mathbf{L}}\mathbf{O}^\top + 2\eta\hat{\mathbf{D}}\right) \\
&\cdot \left(2\alpha\mathbf{I} + 2\gamma\mathbf{OO}^\top + 2\eta\mathbf{I}\right)^{-1}.
\end{aligned}
$$

4) **Z-subproblem** is formulated as:

$$
\mathbf{Z}^{k+1} = \arg\min_{\mathbf{Z}} \|\mathbf{Z}\|_* + \frac{\rho}{2}\|\mathbf{Z} - \mathbf{WXO} + \mathbf{\Lambda}/\rho\|_F^2.
$$

The solution has closed-form via the soft-thresholding operator [Rajwade *et al.*, 2013]:

$$
\mathbf{Z}^{k+1} = \mathrm{SVT}_{1/\rho}(\mathbf{WXO} - \mathbf{\Lambda}/\rho).
$$

5) Finally, update the **Lagrange Multipliers**

$$
\mathbf{\Lambda}^{k+1} = \mathbf{\Lambda}^k + \rho(\mathbf{Z} - \mathbf{WXO}),
$$

and update ρ by $\mu\rho$ for some $\mu > 1$.

4 Theoretical Analysis

We first analyze the convergence of the above algorithm in solving the proposed BLDL model.

Theorem 1. *All these iterative solutions* $\mathbf{W}, \mathbf{O}, \mathbf{D}, \mathbf{Z}, \mathbf{\Lambda}$ *generated by the above ADMM procedure are bounded and convergent.*

We then establish the generalization error bound for the proposed BLDL framework.

Theorem 2. *The generalization error of the model, defined as* $\mathcal{E}_{gen} = \mathbb{E}_\mathcal{D}\left[\|\mathbf{WX} - \mathbf{D}_{true}\|_F^2\right]$, *which is bounded as follows:*

$$
\mathcal{E}_{gen} \leq \frac{\delta_4^2}{1-\delta} + (\delta_3 + \epsilon)^2 + \mathcal{O}\left(\frac{rank(\mathbf{WXO})}{\sqrt{n}}\right),
$$

where δ_4 *is the upper bound imposed by the optimization constraint,* δ *is the Restricted Isometry Property (RIP) constant,* δ_3 *bounds the deviation between* $\mathbf{D}$ *and* $\hat{\mathbf{D}}$, *and* $\mathcal{O}\left(\frac{rank(\mathbf{WXO})}{\sqrt{n}}\right)$ *accounts for the complexity induced by nuclear norm regularization.*

According to this theorem, it ensures that the recovered label distribution is robust to noise, consistent with biased observations, and achieves model simplicity via low-rank constraints. All the proof detail can be found in the appendix.

ID	Data sets	Objects	Features	Labels
1	Flickr	6690	200	8
2	Twitter	6027	200	8
3	Emotion6	1980	12	7
4	Fbp5500	5500	512	5
5	SCUT-FBP	1500	300	5
6	RAF-ML	4908	200	6
7	Gene	17892	36	68
8	Scene	2000	294	9
9	SBU-3DFE	2500	243	6
10	SJAFFE	213	243	6
11	Spo5	2465	24	3
12	Spoem	2465	24	2

Table 1: Details of the datasets

5 Experiments

5.1 Datasets

We evaluate our proposed method on 12 real-world datasets. The datasets cover diverse domains: *Flickr*, *Twitter* [Yang *et al.*, 2017], and *Emotion6* [Peng *et al.*, 2015] describe emotional responses to images. *Fbp5500* and *SCUT-FBP* focus on facial beauty perception [Ren and Geng, 2017]. *RAF-ML* is a text dataset for sentiment analysis [Li and Deng, 2019]. The *Gene* dataset analyzes relationships between genes and diseases [Yu *et al.*, 2012]. *Scene* is derived from a multi-label dataset by converting label rankings into label distributions [Geng and Xia, 2014]. *SJAFFE* and *SBU-3DFE* are facial emotion datasets collected from JAFFE [Lyons *et al.*, 1998] and BU-3DFE [Yin *et al.*, 2006], respectively. Finally, *Spo5* and *Spoem* are yeast datasets obtained from biological experiments [Geng, 2016].

5.2 Evaluation Metrics:

We employ six metrics [Kou *et al.*, 2025] to evaluate the performance of all LDL methods: Chebyshev distance (Chebyshev↓), Clark distance (Clark↓), Kullback-Leibler divergence (KL↓), Canberra metric (Canberra↓), intersection similarity (Intersection↑), and cosine coefficient (Cosine↑).

5.3 Biased LDL Generation:

We simulate biased label distributions by modeling experts' annotations as a voting process, consistent with the Central Limit Theorem. Specifically, Gaussian noise $\left(0, \frac{C}{m}\right)$ is added to the true label distributions, followed by normalization to ensure the distribution constraint holds. Here, m denotes the number of labels, and C controls the deviation degree of the biased label distributions. In our experiments, C is set to 0.1, 0.2, and 0.3 to evaluate varying levels of bias. Parameter C was set to 0.1, 0.2, and 0.3.

5.4 Comparing Methods

We compare our proposed method with seven state-of-the-art LDL methods, briefly introduced as follows:

- **DN-ILDL** [Kou *et al.*, 2024a]: Handles label-dependent and instance-dependent noise by utilizing linear mappings, group sparsity, and graph regularization.

- **LDL-SCL** [Zheng *et al.*, 2018]: Explores local sample correlations through the construction of a local correlation vector.

- **LDLLC** [Jia *et al.*, 2018]: Captures label correlations via a distance-based mapping function.

- **LRS-LDL** [Kou *et al.*, 2023]: Learns a low-rank linear mapping for ground truth and a sparse mapping for noise.

- **LDLLDM** [Wang and Geng, 2021]: Models both global and local label correlations by learning the underlying manifold structure of label distributions.

- **EDL-LRL** [Jia *et al.*, 2019]: Utilizes local label correlations to effectively capture varying intensities of multiple emotions.

- **TLRLDL** [Kou *et al.*, 2024b]: Integrates an auxiliary multi-label learning process within LDL to capture low-rank label correlations.

The hyperparameters setting. The hyperparameters for all methods were set according to their respective publications. For BLDL, the parameters α, β, γ, λ_1, and λ_2 were fine-tuned over the range {0.1, 0.05, 0.01, 0.005, 0.001}. The parameter η was selected from {1, 10, 50, 100, 150}, and T was fixed at 0.5. Each method was evaluated using ten-fold cross-validation to ensure robustness.

5.5 Results and Discussion

Table 2 shows the experimental results (mean±std) of various methods on eight datasets for Clark and Cosine metrics. For $C = 0.1$, the Friedman test [Demšar, 2006] rejected the null hypothesis that "all methods perform equally" (Table 3). Subsequently, the Bonferroni–Dunn test [Demšar, 2006] was used to compare BLDL with others, where methods differing by more than one Critical Difference (CD) are considered significantly different. CD diagrams in Fig. 3 highlight methods within one CD of BLDL connected by a thin line, confirming BLDL's significant advantage. From these results, we conclude:

- **Top-1 dominance.** BLDL achieves top-1 performance in *85.42% (41/48)* of all configurations and consistently ranks first across all metrics by effectively addressing *bias* in the learning process.

- **Benefit of joint modeling.** Compared to methods focusing solely on label correlations (e.g., LDLLC, LDLLDM), BLDL performs better since those methods ignore the *bias* present in label distributions.

- **Superiority over bias-only approaches.** BLDL also outperforms methods that address *bias* alone (e.g., DN-ILDL, LRS-LDL) by additionally leveraging label correlations—an exploit these bias-only methods fail to capture effectively.

5.6 Ablation Study

To validate the proposed method, we design two ablated versions: **(i)** *BLDL-a*: Removes the multi-label recovery process (i.e. drops the first term in Eq. (3)). **(ii)***BLDL-b*: Replaces the

	C	Metric	BLDL	DN-ILDL	LDL-SCL	LDLLC	LRS-LDL	LDLDM	EDL-LDL	TLRLDL
Fli	0.1	Clark	**2.1146±.0020**	2.1990±.0008	2.1576±.0001	2.1990±.0042	2.2029±.0028	2.1705±.0001	2.1797±.0001	2.1777±.0005
		Cosine	**0.8368±.0003**	0.5516±.0002	0.7356±.0001	0.5781±.0038	0.5537±.0005	0.6964±.0001	0.7436±.0001	0.6421±.0009
	0.2	Clark	**2.1175±.0010**	2.1969±.0153	2.1587±.0001	2.1984±.0021	2.1984±.0078	2.1707±.0001	2.1758±.0001	2.1768±.0020
		Cosine	**0.8316±.0034**	0.5531±.0052	0.7289±.0001	0.5781±.0004	0.5556±.0027	0.6869±.0001	0.7414±.0001	0.6356±.0006
	0.3	Clark	**2.1382±.0010**	2.2018±.0033	2.1597±.0001	2.1990±.0019	2.1985±.0028	2.1713±.0001	2.1733±.0001	2.1778±.0005
		Cosine	**0.8276±.0021**	0.5510±.0017	0.7228±.0001	0.5761±.0008	0.5554±.0001	0.6792±.0001	0.7394±.0001	0.6322±.0014
Twi	0.1	Clark	**2.2517±.0028**	2.4072±.0037	2.3602±.0001	2.3957±.0039	2.4043±.0040	2.3656±.0001	2.3874±.0001	2.3726±.0001
		Cosine	**0.8582±.0025**	0.4955±.0013	0.7537±.0001	0.5617±.0022	0.5000±.0008	0.7519±.0001	0.8134±.0001	0.6283±.0004
	0.2	Clark	**2.2783±.0113**	2.4014±.0008	2.3608±.0001	2.3897±.0036	2.4015±.0020	2.3651±.0001	2.3827±.0001	2.3763±.0069
		Cosine	**0.8535±.0015**	0.4980±.0009	0.7509±.0001	0.5621±.0043	0.5016±.0017	0.7372±.0001	0.8124±.0001	0.6211±.0037
	0.3	Clark	**2.3051±.0080**	2.4043±.0050	2.3616±.0001	2.3906±.0034	2.4016±.0020	2.3657±.0001	2.3790±.0001	2.3780±.0017
		Cosine	**0.8480±.0012**	0.4957±.0018	0.7447±.0001	0.5575±.0029	0.5014±.0016	0.7274±.0001	0.8106±.0001	0.6131±.0003
Emo	0.1	Clark	**1.6237±.0067**	1.6753±.0032	1.6457±.0001	1.6875±.0077	1.6820±.0113	1.6404±.0002	1.6423±.0001	1.6697±.0114
		Cosine	0.7462±.0099	0.6592±.0008	0.7266±.0001	0.6700±.0005	0.6560±.0047	0.7417±.0001	**0.7639±.0001**	0.6841±.0020
	0.2	Clark	**1.6408±.0008**	1.6716±.0174	1.6480±.0001	1.6840±.0106	1.6774±.0031	1.6432±.0002	1.6412±.0002	1.6677±.0020
		Cosine	0.7499±.0004	0.6613±.0042	0.7227±.0001	0.6701±.0063	0.6565±.0005	0.7370±.0001	**0.7589±.0001**	0.6816±.0009
	0.3	Clark	**1.6295±.0004**	1.6753±.0051	1.6491±.0001	1.6848±.0104	1.6775±.0031	1.6467±.0001	1.6402±.0002	1.6799±.0001
		Cosine	0.7458±.0030	0.6579±.0004	0.7193±.0001	0.6685±.0059	0.6564±.0005	0.7304±.0001	**0.7574±.0001**	0.6771±.0014
Fbp	0.1	Clark	**1.2494±.0047**	1.5052±.0013	1.4032±.0001	1.4866±.0010	1.5039±.0041	1.4391±.0001	1.3360±.0001	1.6697±.0021
		Cosine	**0.9342±.0010**	0.6571±.0005	0.8596±.0001	0.6772±.0035	0.6617±.0014	0.7929±.0001	0.9169±.0001	0.6841±.0004
	0.2	Clark	**1.2974±.0024**	1.5054±.0021	1.4115±.0001	1.4891±.0001	1.5027±.0003	1.4475±.0001	1.3472±.0001	1.4579±.0015
		Cosine	**0.9264±.0012**	0.6571±.0003	0.8478±.0001	0.6754±.0026	0.6625±.0009	0.7795±.0001	0.9127±.0001	0.7619±.0027
	0.3	Clark	**1.3084±.0053**	1.5040±.0009	1.4182±.0001	1.4895±.0003	1.5028±.0003	1.4530±.0001	1.3542±.0001	1.4623±.0004
		Cosine	**0.9251±.0007**	0.6577±.0004	0.8367±.0001	0.6747±.0022	0.6622±.0009	0.7695±.0001	0.9083±.0001	0.7553±.0005
Scu	0.1	Clark	**1.3869±.0051**	1.4955±.0044	1.4494±.0001	1.4838±.0056	1.4985±.0031	1.4265±.0001	1.3908±.0001	1.4735±.0036
		Cosine	**0.8409±.0075**	0.6647±.0016	0.7775±.0001	0.6717±.0068	0.6672±.0008	0.8089±.0001	0.8405±.0001	0.7217±.0028
	0.2	Clark	**1.3936±.0090**	1.4930±.0037	1.4540±.0001	1.4796±.0055	1.4999±.0003	1.4357±.0001	1.3965±.0001	1.4723±.0045
		Cosine	0.8344±.0013	0.6653±.0013	0.7761±.0001	0.6687±.0056	0.6665±.0018	0.7965±.0001	**0.8369±.0001**	0.7213±.0010
	0.3	Clark	**1.3934±.0066**	1.4971±.0049	1.4562±.0001	1.4807±.0048	1.5001±.0005	1.4394±.0001	1.4022±.0001	1.4748±.0005
		Cosine	**0.8341±.0032**	0.6634±.0013	0.7683±.0001	0.6669±.0069	0.6662±.0019	0.7908±.0001	0.834±.0001	0.7131±.0025
Raf	0.1	Clark	**1.3864±.0003**	1.6119±.0037	1.5534±.0001	1.6115±.0027	1.6102±.0012	1.6025±.0001	1.5410±.0001	1.5688±.0031
		Cosine	**0.8734±.0006**	0.6413±.0006	0.7433±.0001	0.6360±.0011	0.6455±.0001	0.6541±.0001	0.7580±.0001	0.7200±.0011
	0.2	Clark	**1.4205±.0050**	1.6082±.0005	1.5586±.0001	1.6071±.0021	1.6043±.0034	1.6015±.0001	1.5464±.0001	1.5723±.0052
		Cosine	**0.8630±.0007**	0.6418±.0006	0.7349±.0001	0.6356±.0031	0.6472±.0018	0.6566±.0001	0.7506±.0001	0.7153±.0016
	0.3	Clark	**1.4270±.0019**	1.6098±.0005	1.5638±.0001	1.6076±.0019	1.6044±.0033	1.6034±.0001	1.5496±.0001	1.5711±.0001
		Cosine	**0.8519±.0010**	0.6417±.0001	0.7260±.0001	0.6352±.0029	0.6469±.0018	0.6532±.0001	0.7469±.0001	0.7103±.0022
Gen	0.1	Clark	**2.1149±.0179**	2.1151±.0006	2.1230±.0001	2.1618±.0087	2.1222±.0069	2.1248±.0001	2.1240±.0003	2.1312±.0030
		Cosine	**0.8353±.0023**	0.8342±.0003	0.8337±.0001	0.8196±.0006	0.8342±.0009	0.8338±.0001	0.8339±.0001	0.8317±.0005
	0.2	Clark	**2.1228±.0107**	2.1246±.0066	2.1237±.0001	2.1591±.0018	2.1256±.0222	2.1245±.0001	2.1236±.0001	2.1312±.0127
		Cosine	**0.8340±.0016**	0.8336±.0021	0.8333±.0001	0.8202±.0014	0.8334±.0028	0.8337±.0001	0.8338±.0001	0.8329±.0016
	0.3	Clark	**2.1225±.0035**	2.1269±.0035	2.1225±.0005	2.1591±.0018	2.1256±.0222	2.1249±.0006	2.1240±.0005	2.1296±.0187
		Cosine	**0.8338±.0003**	0.8335±.0007	0.8333±.0001	0.8202±.0014	0.8334±.0028	0.8336±.0001	0.8337±.0001	0.8334±.0012
Sce	0.1	Clark	2.4900±.0012	2.4848±.0017	**2.4654±.0001**	2.4915±.0019	2.4747±.0012	2.4702±.0001	2.4775±.0001	2.4736±.0001
		Cosine	**0.7037±.0045**	0.5748±.0003	0.6770±.0001	0.5572±.0008	0.5806±.0013	0.6431±.0001	0.6500±.0001	0.6253±.0007
	0.2	Clark	2.4808±.0129	2.4829±.0001	**2.4668±.0001**	2.4950±.0066	2.4819±.0059	2.4711±.0001	2.4751±.0001	2.4771±.0040
		Cosine	**0.7010±.0010**	0.5753±.0007	0.6692±.0001	0.5553±.0018	0.5780±.0029	0.6367±.0001	0.6469±.0001	0.6205±.0034
	0.3	Clark	2.5100±.0123	2.4859±.0057	**2.4683±.0001**	2.4951±.0066	2.4820±.0059	2.4721±.0002	2.4758±.0001	2.4799±.0040
		Cosine	**0.6876±.0026**	0.5738±.0034	0.6611±.0001	0.5551±.0016	0.5779±.0030	0.6328±.0001	0.6455±.0001	0.6168±.0029
top-1 times			**41**	0	3	0	0	0	4	0

Table 2: Results (mean±std) of the comparing methods in terms of two metrics on ID.1-8 datasets (each is denoted by its first three letters), where the best results are bolded.
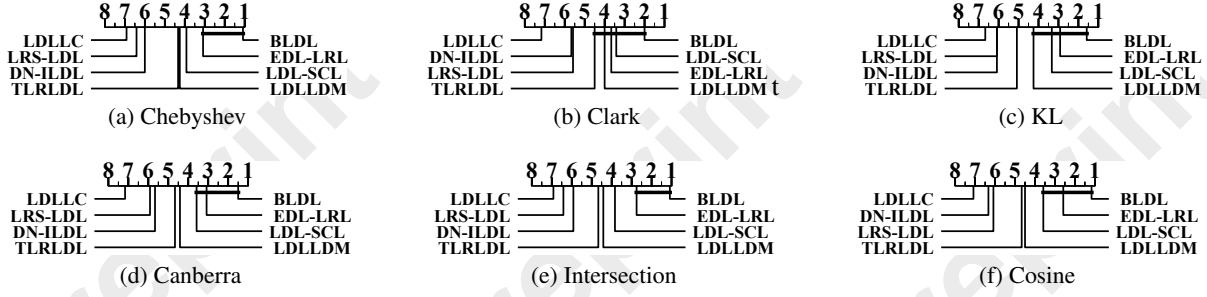
Figure 3: CD diagrams of the comparing methods in terms of each metrics. For the tests, CD equals 2.3296 at 0.05 signifcance level.

Critical Value ($\alpha = 0.05$)	Evaluation metric	Cheb	Clark	KL	Canber	Intersec	Cosine
2.1310	Friedman Statistics F_F	17.6522	8.2619	12.6744	12.5264	19.2706	22.4616

Table 3: The Friedman statistics F_F in terms of six evaluation metrics, as well as the critical value at a significance level of 0.05 (8 algorithms on 12 datasets).
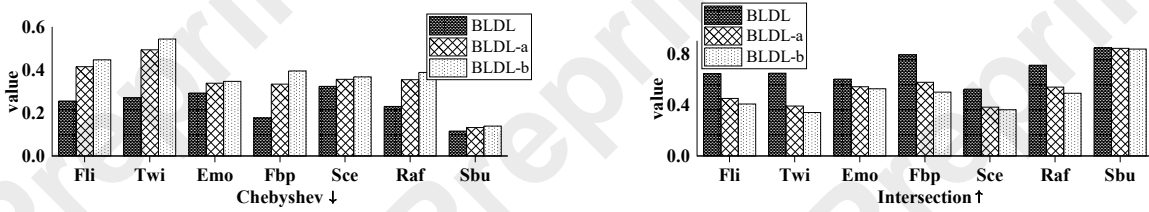
Figure 4: Ablation results on seven datasets in terms of Chebyshev ↓, Intersection ↑.

BLDL *vs*.	Chebyshev	Clark	KL	Canberra	Intersection	Cosine
BLDL-a	**win**[4.88e-04]	**win**[3.42e-03]	**win** [4.88e-04]	**win**[4.88e-04]	**win**[4.88e-04]	**win**[4.88e-04]
BLDL-b	**win**[9.77e-04]	**win** [9.28e-03]	**win**[5.37e-03]	**win**[4.88e-04]	**win** [9.77e-04]	**win**[4.88e-04]

Table 4: The results (Win/Tie/Loss[p-value]) of the Wilcoxon signed-rank tests for BLDL against BLDL-a and BLDL-b at a confidence level of 0.05.

low-rank constraint on $\mathbf{WXO}$ with one on $\mathbf{WO}$, thus applying low-rank modeling in the label-distribution space instead of the multi-label feature space.

We compare BLDL-a and BLDL-b with the full BLDL using biased label distributions generated with $C = 0.1$. Fig. 4 shows results on seven datasets for Chebyshev and Intersection metrics. Wilcoxon signed-rank tests [Demšar, 2006] confirm the statistical significance of BLDL over both ablated versions (Table 4). From these experiments, we draw three key observations:

- **Importance of multi-label recovery.** Comparing BLDL-a vs. BLDL reveals a significant performance drop when the multi-label recovery step is removed, underscoring the critical role of leveraging multiple pseudo-labels to denoise and recover true distributions.

- **Effect of low-rank constraint location.** Comparing BLDL-b vs. BLDL shows that enforcing low-rank structure on $\mathbf{WXO}$ (the recovered multi-label space) outperforms constraining $\mathbf{WO}$ alone, since the multi-label embedding $\mathbf{X}$ is intrinsically low-rank and more robust to annotation noise.

- **Combined benefits.** The full BLDL, which both recovers multi-label distributions and constrains the low-rank structure in the correct space, consistently achieves the best results across all metrics and datasets.

5.7 Validation of Hypothesis

We computed the difference between the recovered label distribution and the biased label distribution during the training phase, denoted as δ_1, and the difference between the multi-label corresponding to the recovered label distribution and the multi-label corresponding to the biased distribution, denoted as δ_2. As show in Fig. 5, it can be observed that δ_1 is consistently greater than δ_2 until convergence. Therefore, during the label distribution recovery phase, multi-label information is more reliable than the biased label distribution information.

5.8 Analysis of Label Distribution Recovery

We evaluate the recovery error of label distributions during training using the Frobenius norm $\|D_{\text{recover}} - D_{\text{truth}}\|_F$, as shown in Fig. 6. Our method achieves lower recovery error
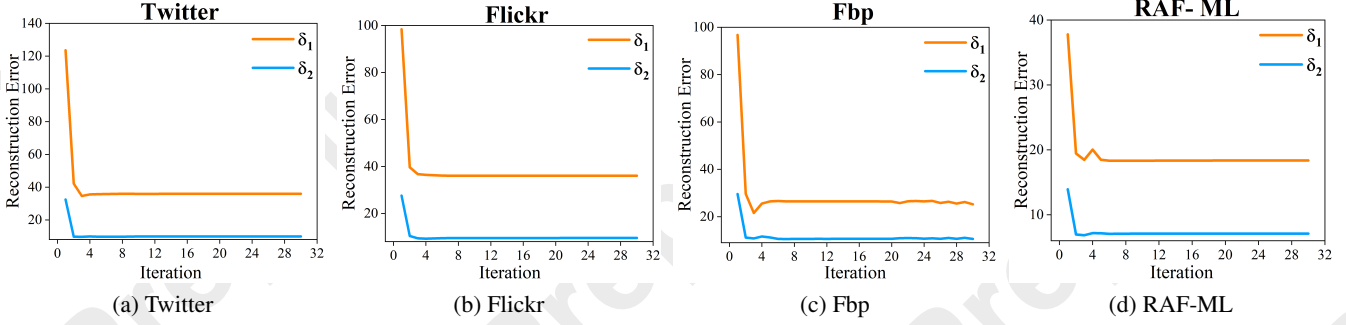
Figure 5: Error reduction (δ_1 and δ_2) during iterations on four datasets: (a) Twitter, (b) Flickr, (c) Fbp, and (d) RAF-ML.
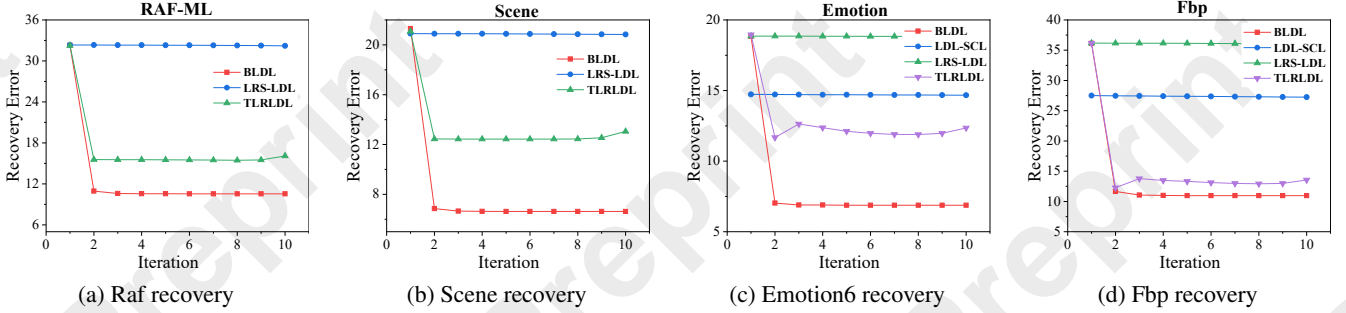

Figure 6: Reconstruction error in recovering true distributions for different methods during the traning stage.
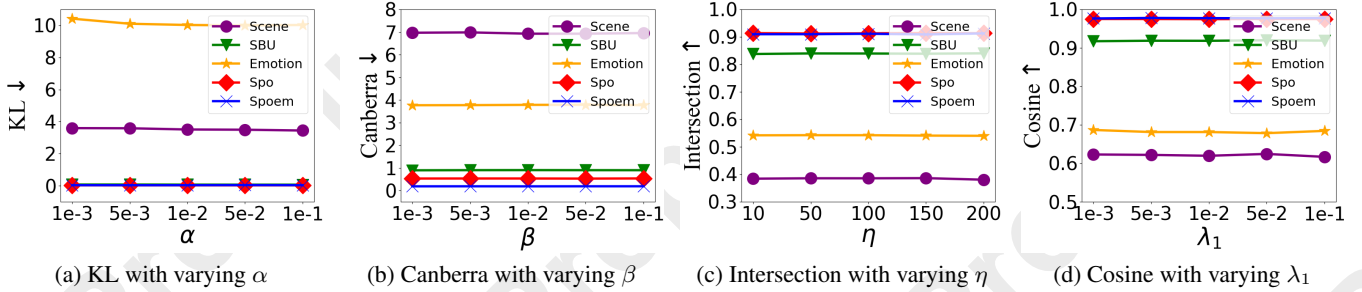

Figure 7: The performance of BLDL with varying parameters in terms of four different metrics on five datasets.

compared to LRS-LDL, demonstrating the benefit of leveraging multi-label information. Additionally, it outperforms TL-RLDL by addressing biases in the learning process, further improving recovery accuracy.

5.9 Parameter Sensitivity Analysis

We analyze the sensitivity of $\alpha, \beta, \eta, \lambda_1$, with α, β, λ_1 chosen from $\{0.1, 0.05, 0.01, 0.005, 0.001\}$ and η from $\{1, 10, 50, 100, 150\}$. Experiments on five datasets (Scene, SBU, Emotion, Spo, Spoem) show in Fig. 7 that BLDL exhibits stable performance, demonstrating robustness to parameter variations.

6 Conclusion

This paper introduces a novel framework, Biased Label Distribution Learning (BLDL), to address label distribution learning under biased annotations. Unlike conventional methods, BLDL first converts biased soft label distributions into multi-label representations, effectively mitigating annotation noise and bias. It further exploits the intrinsic low-rank structure of multi-label spaces to reliably recover true label distributions. Comprehensive theoretical analysis and experiments on diverse real-world datasets demonstrate that BLDL significantly enhances the accuracy and robustness of label distribution recovery, outperforming state-of-the-art methods.

Acknowledgments

References

[Boyd *et al.*, 2011] Stephen Boyd, Neal Parikh, Eric Chu, Borja Peleato, and Jonathan Eckstein. 2011.

[Demšar, 2006] Janez Demšar. Statistical comparisons of classifiers over multiple data sets. *The Journal of Machine learning research*, 7:1–30, 2006.

[Geng and Xia, 2014] Xin Geng and Yu Xia. Head pose estimation based on multivariate label distribution. In *Proceedings of the IEEE conference on computer vision and pattern recognition*, pages 1837–1842, 2014.

[Geng, 2016] Xin Geng. Label distribution learning. *IEEE Transactions on Knowledge and Data Engineering*, 28(7):1734–1748, 2016.

[Gu *et al.*, 2014] Shuhang Gu, Lei Zhang, Wangmeng Zuo, and Xiangchu Feng. Weighted nuclear norm minimization with application to image denoising. In *Proceedings of the IEEE conference on computer vision and pattern recognition*, pages 2862–2869, 2014.

[He *et al.*, 2024] Liang He, Yunan Lu, Weiwei Li, and Xiuyi Jia. Generative calibration of inaccurate annotation for label distribution learning. In *Proceedings of the AAAI Conference on Artificial Intelligence*, volume 38, pages 12394–12401, 2024.

[Huang and Zhou, 2012] Sheng-Jun Huang and Zhi-Hua Zhou. Multi-label learning by exploiting label correlations locally. In *Proceedings of the AAAI Conference on Artificial Intelligence*, volume 26, pages 949–955, 2012.

[Jia *et al.*, 2018] Xiuyi Jia, Weiwei Li, Junyu Liu, and Yu Zhang. Label distribution learning by exploiting label correlations. In *Proceedings of the AAAI Conference on Artificial Intelligence*, volume 32, 2018.

[Jia *et al.*, 2019] Xiuyi Jia, Xiang Zheng, Weiwei Li, Changqing Zhang, and Zechao Li. Facial emotion distribution learning by exploiting low-rank label correlations locally. In *Proceedings of the IEEE/CVF Conference on computer vision and pattern recognition*, pages 9841–9850, 2019.

[Jing *et al.*, 2016] Xiao-Yuan Jing, Fei Wu, Zhiqiang Li, Ruimin Hu, and David Zhang. Multi-label dictionary learning for image annotation. *IEEE Transactions on Image Processing*, 25(6):2712–2725, 2016.

[Kou *et al.*, 2023] Zhiqiang Kou, Jing Wang, Yuheng Jia, Biao Liu, and Xin Geng. Instance-dependent inaccurate label distribution learning. *IEEE Transactions on Neural Networks and Learning Systems*, 2023.

[Kou *et al.*, 2024a] Zhiqiang Kou, Jing Wang, Yuheng Jia, and Xin Geng. Inaccurate label distribution learning with dependency noise. *arXiv preprint arXiv:2405.16474*, 2024.

[Kou *et al.*, 2024b] Zhiqiang Kou, Jing Wang, Jiawei Tang, Yuheng Jia, Boyu Shi, and Xin Geng. Exploiting multi-label correlation in label distribution learning. In *IJCAI*, pages 4326–4334, 2024.

[Kou *et al.*, 2025] Zhiqiang Kou, Jing Wang, Yuheng Jia, and Xin Geng. Progressive label enhancement. *Pattern Recognition*, 160:111172, 2025.

[Li and Deng, 2019] Shan Li and Weihong Deng. Blended emotion in-the-wild: Multi-label facial expression recognition using crowdsourced annotations and deep locality feature learning. *International Journal of Computer Vision*, 127(6):884–906, 2019.

[Liu *et al.*, 2017] Jingzhou Liu, Wei-Cheng Chang, Yuexin Wu, and Yiming Yang. Deep learning for extreme multi-label text classification. In *Proceedings of the 40th international ACM SIGIR conference on research and development in information retrieval*, pages 115–124, 2017.

[Lyons *et al.*, 1998] Michael Lyons, Shigeru Akamatsu, Miyuki Kamachi, and Jiro Gyoba. Coding facial expressions with gabor wavelets. In *Proceedings Third IEEE international conference on automatic face and gesture recognition*, pages 200–205, 1998.

[Peng *et al.*, 2015] Kuan-Chuan Peng, Tsuhan Chen, Amir Sadovnik, and Andrew C Gallagher. A mixed bag of emotions: Model, predict, and transfer emotion distributions. In *Proceedings of the IEEE conference on computer vision and pattern recognition*, pages 860–868, 2015.

[Rajwade *et al.*, 2013] Ajit Rajwade, Anand Rangarajan, and Arunava Banerjee. Image denoising using the higher order singular value decomposition. *IEEE Transactions on Pattern Analysis and Machine Intelligence*, 35(4):849–862, 2013.

[Ren and Geng, 2017] Yi Ren and Xin Geng. Sense beauty by label distribution learning. In *IJCAI*, pages 2648–2654, 2017.

[Wang and Geng, 2021] Jing Wang and Xin Geng. Label distribution learning by exploiting label distribution manifold. *IEEE transactions on neural networks and learning systems*, 34(2):839–852, 2021.

[Xie and Huang, 2018] Ming-Kun Xie and Sheng-Jun Huang. Partial multi-label learning. In *Proceedings of the AAAI conference on artificial intelligence*, volume 32, 2018.

[Xu and Zhou, 2017] Miao Xu and Zhi-Hua Zhou. Incomplete label distribution learning. In *IJCAI*, pages 3175–3181, 2017.

[Yang *et al.*, 2017] Jufeng Yang, Ming Sun, and Xiaoxiao Sun. Learning visual sentiment distributions via augmented conditional probability neural network. In *Proceedings of the AAAI Conference on Artificial Intelligence*, volume 31, 2017.

[Yin *et al.*, 2006] Lijun Yin, Xiaozhou Wei, Yi Sun, Jun Wang, and Matthew J Rosato. A 3d facial expression database for facial behavior research. In *7th international conference on automatic face and gesture recognition (FGR06)*, pages 211–216, 2006.

[Yu *et al.*, 2012] Jia-Feng Yu, Dong-Ke Jiang, Ke Xiao, Yun Jin, Ji-Hua Wang, and Xiao Sun. Discriminate the falsely predicted protein-coding genes in aeropyrum pernix k1 genome based on graphical representation. *Match-Communications in Mathematical and Computer Chemistry*, 67(3):845, 2012.

[Zhang and Zhou, 2014] Min-Ling Zhang and Zhi-Hua Zhou. A review on multi-label learning algorithms. *IEEE Transactions on Knowledge and Data Engineering*, 26(8):1819–1837, 2014.

[Zheng *et al.*, 2018] Xiang Zheng, Xiuyi Jia, and Weiwei Li. Label distribution learning by exploiting sample correlations locally. In *Proceedings of the AAAI Conference on Artificial Intelligence*, volume 32, 2018.

[Zhu *et al.*, 2017] Yue Zhu, James T Kwok, and Zhi-Hua Zhou. Multi-label learning with global and local label correlation. *IEEE Transactions on Knowledge and Data Engineering*, 30(6):1081–1094, 2017.